Nanoscale

MoS2 Exhibits Stronger Toxicity with Increased Exfoliation

Journal:	*Nanoscale*
Manuscript ID:	NR-ART-08-2014-004907.R1
Article Type:	Paper
Date Submitted by the Author:	23-Sep-2014
Complete List of Authors:	Chng, Elaine; Nanyang Technological University, Chemistry and Biological Chemistry Sofer, Zdenek; Institute of Chemical Technology, Prague, Department of Inorganic Chemistry Pumera, Martin; Nanyang Technological University, Chemistry and Biological Chemistry

Journal Name

RSCPublishing

ARTICLE

MoS_2 Exhibits Stronger Toxicity with Increased Exfoliation

Cite this: DOI: 10.1039/xoxxoooooox

Elaine Lay Khim Chng[a], Zdeněk Sofer[b], Martin Pumera[a]*

Received ooth January 2012,
Accepted ooth January 2012

DOI: 10.1039/xoxxoooooox

www.rsc.org/

MoS_2 belong to a class of inorganic 2D nanomaterial known as transition metal dichalcogenides (TMDs) which have recently seen a renewed and growing interest due to their interesting electronic and catalytic properties when scaled down to single or few layer sheets. Although exfoliated MoS_2 nanosheets have been proposed for numerous energy-related and biosensing applications, little is known about the toxicological impacts of using MoS_2 nanosheets. Here, we report about the *in-vitro* toxicity of MoS_2 nanosheets that has been chemically exfoliated with different lithium intercalating agents and compared their respective cytotoxic influence. Methyllithium (Me-Li), *n*-butyllithium (*n*-Bu-Li) and *tert*-buthyllithium (*t*-Bu-Li) were used for the exfoliation of bulk MoS_2 and we found the *t*-Bu-Li and *n*-Bu-Li exfoliated MoS_2 nanosheets to be more cytotoxic than MoS_2 exfoliated by Me-Li. Characterization confirmed that *t*-Bu-Li and *n*-Bu-Li provide more efficient exfoliation over Me-Li, we establish that the extent of exfoliation that MoS_2 undergoes is a factor influencing their toxicity. Specifically, the more exfoliated the MoS_2 nanosheets, the stronger its cytotoxic influence; which may be due to an increase in surface area and active edge sites. The potential toxicity of these MoS_2 nanosheets should be taken into account before their employment in real world applications and we have shown the effect of the amount of exfoliation can have on their toxicity of MoS_2 nanosheets, representing the first step towards a better understanding of their toxicological properties.

Introduction

Two-dimensional (2D) nanomaterials have been rapidly gaining momentum in the area of nanoscience in recent years and leading this development is the widely studied nanomaterial – graphene. The remarkable properties demonstrated by graphene have led to the pursuit of other inorganic, 2D nanomaterials that can be derived from layered bulk forms that are similar to graphite.[1-3] There has been a growing interest on another class of 2D materials known as the transition metal dichalcogenides (TMDs). TMDs are considered as another category of inorganic layered compound with a general formula MX_2, where M is a transition metal element from (Ti, Zr, V, Ta, Mo, W, etc.) and X is a chalcogen (S, Se, Te). In the same manner as graphite, TMDs form layered structures where the atoms are covalently bonded in the X−M−X configuration into nanosheets, stacking to form three-dimensional crystal structures *via* weak van der Waals' interactions.[4]

In particular, molybdenum disulfide (MoS_2) which is seen as a graphene analogue with a structure consisting of chemically bonded 2D S−Mo−S layers held together by van der Waals' interactions,[5,6] has been shown to surpass graphene and other commonly used silicon-based materials in electronic applications and energy-harvesting systems.[7-12] More importantly, MoS_2 has recently emerged as a potential candidate for applications in sensing[13] and energy generation[14] platforms. The electrochemical sensing behaviour of MoS_2 has been reported in which the reduction of single-layer MoS_2 nanosheets were used in glucose sensing, and in the selective detection of dopamine in the presence of uric acid and ascorbic acid.[15] In addition, functionalized MoS_2 nanosheets have been employed to immobilize DNA strands and immunoglobins for biosensing applications as well[16,17] or to act as DNA labels.[18] The use of such novel inorganic nanomaterials for any bioapplications however, draws concern over its possible toxicological implications.[19] Likewise, given the potential employment of MoS_2 nanosheets towards bioapplications, concerns will arise over their toxicological profiles. And since MoS_2 has a layered structure whereby the number of layers can influence its properties,[20,21] the extent of exfoliation is a crucial factor when fabricating MoS_2 nanosheets. Therefore, the aim of our study is to address the fundamental issue of the *in-vitro* toxicity of MoS_2 nanosheets and examine how the exfoliation of MoS_2 with different intercalating agents can impact its *in-vitro* toxicological behaviour.

Experimental Section

Cell Culture

Human lung carcinoma epithelial cell line A549 was used to determine the toxicity of the nanomaterials. It is a popular cell line in nanotoxicological studies with a cell cycle time of 22 h. A549 cells were purchased from Bio-REV Singapore. Cells were cultured in minimum essential medium (MEM) supplemented with 10% fetal bovine serum (FBS) and 1% penicillin/ streptomycin in an incubator maintained at 37 ˚C under 5% CO_2. Typically, the A549 cells were seeded in 24-well plates at a volume of 570 μL/ well with a cell density of 5×10^4.

Cell Exposure to MoS_2 nanomaterials

Exposure to the nanomaterials were carried out 24 h after the cells were seeded into the 24-well plates. The medium is removed and each well was rinsed with PBS (pH 7.4), Following that, the cells in each well were incubated with 570 μL of the different concentrations of the nanomaterial dispersions. The cells were exposed to the nanomaterial dispersions for 24 h. Cells without nanomaterials exposure were used as control.

MTT Assay – Cellular Viability

In MTT assays the 3-(4,5-dimethylthiazol-2-yl)-2,5-diphenyltetrazolium bromide is reduced to purple formazan, which is water insoluble. For MTT viability measurements, the stock MTT solution was diluted to 1 mg/mL from a stock solution of 5 mg/mL. After 24 h exposure, the cells were washed twice with PBS (pH 7.4) and incubated with the diluted MTT solution (300 μL/ well) at 37 ˚C and 5% CO_2 for 3 h. Finally, the MTT solution was removed and dimethyl sulfoxide (DMSO) was added (300 μL/ well) to dissolve the insoluble purple formazan crystals produced by live cells. The plates were gently agitated for 5 min, after which the assay liquid were transferred into individual eppendorf tubes to be centrifuged at 8000g for 10 min to remove traces of the nanomaterials. 100 μL of the supernatent was then transferred to a 96-well plate to be measured for absorbance at 570 nm, with 690 nm as the background absorbance.

MTT Assay – Particle Interference

The tendency of nanomaterials reacting with the MTT to produce formazan was measured in a cell-free experiment. The nanomaterial dispersions were prepared with the diluted MTT solution and incubated in a 24-well plate at 37 ˚C for 3 h. DMSO was then added in a ratio of 1:1 to the MTT-nanomaterial mixure and was incubated for 10 min at at 37 ˚C. The final mixture was centrifuged at 8000g for 10 min, and the supernatent absorbance was measured at 570 nm, with 690 nm as the background absorbance.

We also investigated if the nanomaterials were able to interfere with the MTT assay by binding to the MTT molecule, preventing its reduction to formazan, or by binding to the formazan product. In the absence of cells, the MTT was reduced to formazan by using ascorbic acid. After the 3 h incubation with the nanomaterials, 0.20 mL of the MTT-nanomaterials mixture (mentioned above) was mixed with 0.12 mL of ascorbic acid (4 mM) and incubated for another hour at 37 ˚C. DMSO was then added to the MTT-nanomaterial-ascorbic acid mixture at a ratio of 2:1 and incubated for 10 min at 37 ˚C. The final mixture was centrifuged at 8000g for 10 min, and the supernatent absorbance was measured at 570 nm, with 690 nm as the background absorbance.

WST-8 Assay – Cellular Viability

Besides the MTT assay, cell viability was also measured by using a water soluble tetrazolium salt, WST-8 assay. For measurements, the stock WST-8 (2-(2-methoxy-4-nitrophenyl)-3-(4-nitrophenyl)-5-(2,4-disulfophenyl)-2H-tetrazolium) solution was diluted at a ratio of 1:10. After 24 h exposure, the cells were washed twice with PBS (pH 7.4) and incubated with the diluted WST-8 solution (300 μL/ well) at 37 ˚C and 5% CO_2 for 1 h. Finally, the assay liquid were transferred into individual eppendorf tubes to be centrifuged at 8000g for 10 min to remove traces of the nanomaterials. 100 μL of the supernatent was then transferred to a 96-well plate to be measured for absorbance at 450 nm, with 800 nm as the background absorbance.

WST-8 Assay – Particle Interference

The nanomaterial dispersions were prepared with the diluted WST solution and subsequently incubated at 37 ˚C for 1 h. After incubation, the mixture was centrifuged at 8000g for 10 min, and the supernatent absorbance was measured at 450 nm, with 800 nm as the background absorbance.

Materials

MoS_2 bulk powder (< 2 μm) was purchased from Sigma–Aldrich, Singapore. Methyllithium (1.6M in diethyl ether), *n*-butyllithium (1.6M in hexane) and *tert*-buthyllithium (1.7M in pentane) were obtained from Aldrich, Czech Republic. Hexane was obtained from Lach-ner, Czech Republic. Argon (99.9999% purity) was obtained from SIAD, Czech Republic.

Procedures

Exfoliation of MoS_2 were carried out by suspending 3 g of MoS_2 bulk powder in 20 ml of 1.6 M methyllithium in diethylether, 20 ml of 1.6 M *n*-butyllithium in hexane, or 20 ml of 1.7 M *tert*-butyllithium in pentane. The solution was stirred for 72 h at 25 °C under argon atmosphere. The Li-intercalated material was then separated by suction filtration under argon atmosphere and the intercalating compound was washed several times with hexane (dried over Na). The separated MoS_2 with intercalated Li was placed in water (100 ml) and repeatedly centrifuged (18 000 g). The final material was dried in vacuum oven at 50 °C for 48 hours prior further use. SEM images of the exfoliated MoS_2 can be found in ref.[22]

Results and discussion

In our present work, we will be focusing on chemical Li-intercalation as it is one of the most widely used method to produce MoS_2 nanosheets.[11] The process primarily consists of intercalating the Li ions between the MoS_2 layers and when the Li reacts with water, this leads to the spontaneous (or aided by ultrasonication) exfoliation of the Li-intercalated MoS_2. Thus, the efficiency of the exfoliation is clearly dependent on the process of Li-intercalation.

Three different organolithium compounds: methyllithium (Me-Li), *n*-butyllithium (*n*-Bu-Li) and *tert*-butyllithium (*t*-Bu-Li) were chosen as the intercalating reagents in the chemical exfoliation of bulk MoS_2. These compounds differ in their sizes and structures so in order to examine the degree of exfoliation undergone by the bulk MoS_2, the MoS_2 nanosheets obtained after the chemical exfoliation were characterized. A comprehensive characterization of the nanomaterials is a necessary component in any toxicological screening tests to better understand the relationship between their properties and the measured toxicity effects. Thus, various techniques including Raman spectroscopy and high-resolution X-ray photoelectron spectroscopy (XPS) were employed.[22]

Table 1. Full widths at half maximum (FWHM) values obtained from Raman and XPS spectra.[22]

	Bulk MoS_2	Me-Li	*n*-Bu-Li	*t*-Bu-Li
FWHM of E_{2g} and A_{1g} (cm^{-1})[a]	6.5	6.5	10.5	10.5
FWHM of Mo $3d_{5/2}$ (eV)[b]	0.93	1.08	1.14	1.17
FWHM of S $2p_{3/2}$ (eV)[b]	0.93	1.18	1.26	1.29

[a]FWHM data obtained from Raman spectroscopy

[b] FWHM data obtained from XPS

The raman spectra for all four samples presented in-plane E_{2g} and out-of-plane A_{1g} vibration modes as two clear peaks at 380 cm^{-1} and 405 cm^{-1}, respectively.[23] The softening and broadening of the E_{2g} and A_{1g} bands can be observed with a corresponding increase in their FWHM from 6.5 cm^{-1} (for bulk and Me-Li) to 10.5 cm^{-1} (*n*-Bu-Li and *t*-Bu-Li). This increment can be correlated to the decrease in the number of MoS_2 nanosheet layers,[1] suggesting that both *n*-Bu-Li and *t*-Bu-Li can better intercalate between the MoS_2 sheets for a more effective exfoliation of the bulk MoS_2, as compared with Me-Li.

In addition, XPS analysis provided elemental composition and bonding information, confirming that all three exfoliated nanosheets and the bulk material have the composition MoS_2. The Mo 3d spectra of the exfoliated samples were observed to be similar to that of the bulk MoS_2, and focusing on the Mo $3d_{5/2}$ band at 229.4 eV, it is noted that the FWHM increased in the order Me-Li < *n*-Bu-Li < *t*-Bu-Li for the exfoliated MoS_2 nanosheets (see Table 1). The increase in FWHM has been correlated to a reduction in particle sizes,[24] making the exfoliation process more favourable. Likewise, zooming into the S 2p region of the exfoliated products, the same increasing trend of Me-Li < *n*-Bu-Li < *t*-Bu-Li can be observed for the FWHM from the S $2p_{3/2}$ signal at 162.3 eV. Hence, it is evident from the analyses of the Raman and XPS data that MoS_2 exfoliation proceeds most efficiently with *t*-Bu-Li as the intercalating agent, followed by *n*-Bu-Li and finally, Me-Li.[22]

The extent of MoS_2 exfoliation has important implications because well-exfoliated nanosheets, from single- to few-layers, offer a higher surface area of edge-terminated sites. This would lead to an enhancement of MoS_2 properties such as capacitive and catalytic behaviours in applications for supercapacitors and hydrogen evolution reaction (HER),[25,26] respectively.

In-vitro Assessments

Next, we move on to the main objective of this study which is to establish the cytotoxicity profiles of the exfoliated MoS_2 nanosheets, and investigate if the use of different organolithium compounds in the exfoliation process will have an impact on their toxicity behaviour.

Biological nanotoxicity assessments represent the first step towards addressing fundamental toxicity issues that may be encountered with such nanomaterials. In our work, to evaluate the dose-response experienced by the *in-vitro* model when exposed to MoS_2 that has been exfoliated with different Li intercalating agents, we chose the human lung carcinoma epithelial (A549) cell line along with two universal viability assays: a) Methylthiazolyldiphenyl-tetrazoliumbromide (MTT), and b) Water-soluble tetrazolium salt (WST-8).

The A549 cells were incubated with suspensions of the Me-Li, *n*-Bu-Li and *t*-Bu-Li exfoliated MoS_2 nanosheets, as well as the bulk MoS_2 material at varying concentrations for 24 h. Thereafter, the viability of the A549 cells was examined using the MTT and WST-8 assays. Figure 1 shows the dose-response data obtained from the MTT assay.

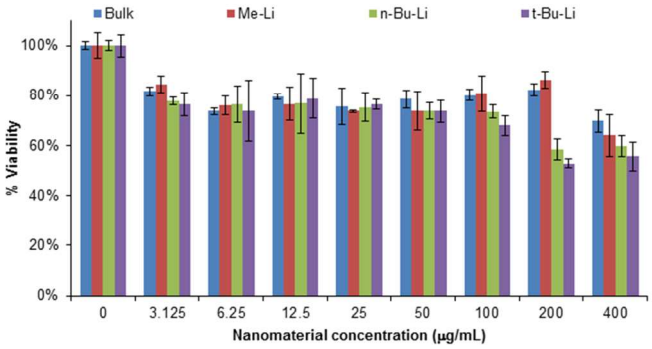

Figure 1. Cytotoxicity assessment following a 24 h exposure to varying concentrations of bulk MoS_2, and after exfoliation with methyllithium (Me-Li), *n*-buthyllithium (*n*-Bu-Li) and *tert*-butyllithium (*t*-Bu-Li). Cell viability of the human lung carcinoma epithelial cells was determined using the MTT assay. Data represent mean ± standard deviation.

The data obtained from the MTT assay presented a dose dependent response from all the four MoS_2 samples across the varying concentrations from 3.125 – 400 μg/mL and starting with the lowest concentration at 3.125 μg/mL, a slight drop in the cell viability can be observed for all the samples. Interestingly, while comparing the potential effects of the different exfoliated MoS_2 nanosheets on the A549 cells, we found little trend in their cytotoxicity profiles given that percentage viability remained relatively constant at approximately 74 – 81% across all four nanomaterials with concentrations from 3.125 to 50 μg/mL. However, at the higher dosages of 100, 200 and 400 μg/mL, the influence of using different intercalating agents becomes clearer as we start observing a trend between the MoS_2 samples.

From the data, we notice that MoS_2 exfoliated with *t*-Bu-Li elicited the strongest toxic response, followed by MoS_2 exfoliated with *n*-Bu-Li and finally Me-Li, suggesting that the extent of exfoliation is a factor influencing the cytotoxicity of these MoS_2 nanosheets. The percentage viability of the cells that were exposed to MoS_2 exfoliated with Me-Li is roughly comparable to the response we see when the cells were exposed to the non-exfoliated, bulk MoS_2. In contrast, the cytotoxic impact on the A549 cells becomes more obvious with *n*-Bu-Li and *t*-Bu-Li exfoliated nanosheets as only 53 – 55% of the cells remained viable at dosages between 200 and 400 μg/mL, as compared to 64 – 82% cell viability observed for Me-Li exfoliated and bulk MoS_2. Accordingly, our MTT data implies that the more exfoliated MoS_2 nanosheets have a stronger cytotoxic effect on the A549 cells, since we have shown from earlier characterizations that both *n*-Bu-Li and *t*-Bu-Li provide a more effective exfoliation over Me-Li.

With the intention of supporting our MTT data, we chose to use another assay that has similar working mechanism as the MTT. The WST-8 is an assay which uses a water-soluble tetrazolium salt, and both assays are colourimetric assessments that provides information on cell viability through a bioreduction process between the viable cells and assay reagent.

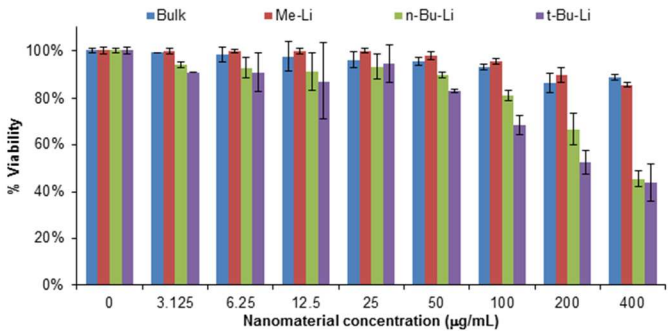

Figure 2. Cytotoxicity assessment following a 24 h exposure to varying concentrations of bulk MoS_2, and after exfoliation with methyllithium (Me-Li), *n*-buthyllithium (*n*-Bu-Li) and *tert*-butyllithium (*t*-Bu-Li). Cell viability of the human lung carcinoma epithelial cells was determined using the WST-8 assay. Data represent mean ± standard deviation.

In Figure 2, whilst a dose-dependent response can be seen from the WST-8 data, it is not an obvious as compared with the MTT data at the earlier concentrations, especially for the Me-Li exfoliated and bulk MoS_2. Despite this, a trend between the different exfoliated MoS_2 nanosheets can already be established even at the lowest concentration of 3.125 μg/mL; wherein their cytotoxicity can be arranged in the order of *t*-Bu-Li > *n*-Bu-Li > MeLi. Specifically, MoS_2 exfoliated with *t*-Bu-Li produced nanosheets which induced the most toxic response from the A549 cells while those exfoliated with Me-Li were the least toxic. In fact at more concentrated dosages of 100 – 400 μg/mL, the WST-8 data showed a high cell viability of 86 – 95% for the Me-Li exfoliated MoS_2 nanosheets, which is incidentally comparable to the response obtained from incubation with the bulk MoS_2 at 86 – 92%. On the other hand, the *n*-Bu-Li and *t*-Bu-Li exfoliated MoS_2 at these concentrations were significantly more cytotoxic with cell viabilities of 45 – 81% and 44 – 68% respectively, which tells us that there is a clear distinction between the toxicity profiles of the *n*-Bu-Li, *t*-Bu-Li exfoliated and the Me-Li exfoliated MoS_2 nanosheets. Therefore, the implications derived from the WST-8 data are in good agreement with the MTT results, in which we find that MoS_2 nanosheets with a greater degree of exfoliation exhibit a much more cytotoxic influence on the A549 cells.

We also conducted appropriate cell-free control experiments which are carried out in the absence of cells to allow us to confirm the viability results obtained from the MTT and WST-8 assays are free of any interference that might be induced by the nanomaterials itself. The reason being the small dimensions and high surface area of these nanomaterials makes them susceptible to interactions with the assay compounds. To illustrate, several reports have shown the active reagent in viability assays interacting with carbon nanomaterials causing either an inflated viability result or a false toxic response.[27-29] To ensure that such occurrence does not have an effect on the data we have obtained in Figures 1 and 2, cell-free control experiments were performed.

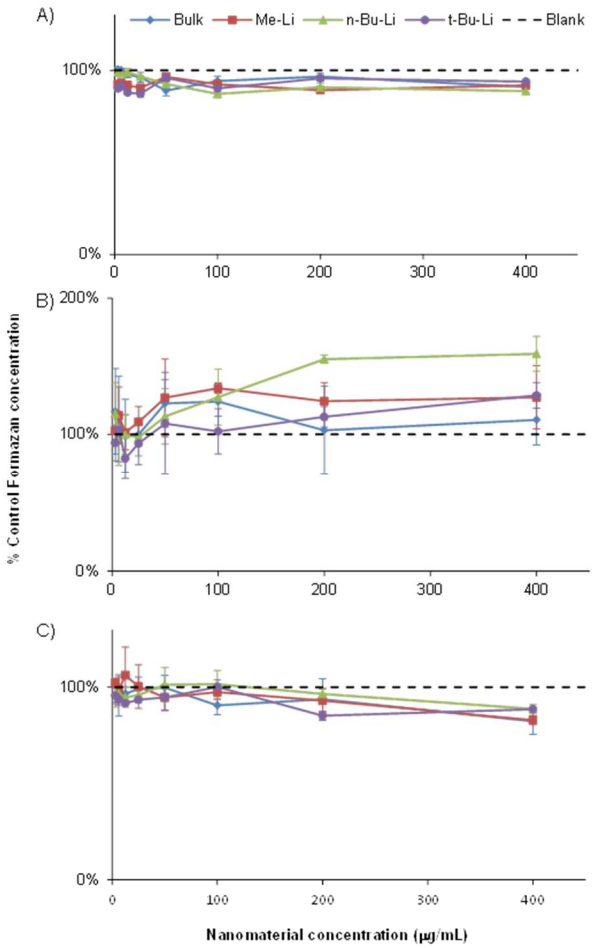

Figure 3. Interference control experiments carried out on the bulk MoS_2, Me-Li, *n*-Bu-Li and *t*-Bu-Li exfoliated MoS_2 under cell-free conditions. Percentage of formazan generated from a) possible generation of formazan product by reacting with WST-8 reagent, b) possible generation of formazan product by reacting with MTT reagent and c) possible binding of tetrazolium salt from MTT reagent. Data represent mean ± standard deviation.

First, we wanted to find out if the MoS_2 nanomaterials are capable of spontaneously reacting with the MTT and WST assay reagents. Monteiro-Riviere *et al.*[22] and Wörle-Knirsch *et al.*[283] have shown carbon-based nanomaterials to be able to reduce the MTT reagent, causing an overestimated measurement of cell viability, potentially covering up a cytotoxic response.

To find out if the MoS_2 nanomaterials are capable of reducing the tetrazolium compound in the dye agents, we carried out control experiments by incubating the four MoS_2 nanomaterials with assay reagents in the absence of cells. Figures 3a and 3b present the results for the WST-8 and MTT assays, respectively. The WST-8 results revealed no indications of the MoS_2 nanomaterials spontaneously reducing the tetrazolium compound as the average formazan percentage is within 90−96% of the normalized MoS_2 -free blank control, but the same cannot be said for the MTT assay.

Even though no cells were present, the MTT control showed added absorbance for all the MoS_2 samples and the effect was more noticeable for the three exfoliated MoS_2 nanosheets at the higher concentrations. At concentrations between 50 – 400 μg/mL, the extra absorbance ranges from 24−34%, 13−55% and 2−29% for the Me-Li, *n*-Bu-Li and *t*-Bu-Li exfoliated MoS_2, respectively. This indicates that the exfoliated MoS_2 nanosheets were able to spontaneously cause a bio-reduction of the MTT reagent, and as a result the MTT assay might not be a suitable assessment to evaluate the toxicity of MoS_2 nanomaterials in this case. With that said, we should clarify that in our procedure (see experimental section), after a 24 h incubation period with the nanomaterials, the cells would be thoroughly rinsed twice with phosphate buffer solution to remove most traces of the MoS_2 nanomaterials before the cells were treated with the MTT dye reagent. This is to ensure that we minimize any potential reaction between the tested materials and the reagent. Thus, the additional absorbance we observe from the control experiments should not have much impact on the MTT cell viability data in Figure 1.

Following that, we needed to find out whether the insoluble crystals from the MTT assay were being adsorbed onto any of the MoS_2 nanomaterials. Note that because the WST-8 assay uses a water soluble tetrazolium salt, it is not necessary to check for possible adsorption. Briefly, viable cells are able to reduce the MTT reagent to give the insoluble formazan and when adsorbed onto the MoS_2 nanomaterials, the subsequent rinsing and centrifuging to remove the nanomaterials will also result in the loss of the adsorbed coloured crystals. This eventually leads to a reduction in the absorbance reading causing a false toxic reponse. For instance, past studies have shown that the insoluble crystals can be adsorbed onto single-walled carbon nanotubes.[28,29]

To test for adsorption, ascorbic acid will be added to the MoS_2 nanomaterials-MTT mixture to reduce the MTT under a cell-free condition to give the insoluble purple crystal. A solubilization step with DMSO follows, along with centrifugation to remove traces of any nanomaterials with their adsorbed formazan crystals, if any. The formazan generated was then normalized against the nanomaterials-free blank, *i.e.* the MTT-ascorbic acid mixture. From Figure 3c, the average formazan generated is 82−99% of the normalized blank reading and the lower limit is based on 400 μg/mL of the MoS_2 nanomaterials. Hence, a small amount of the formazan crystal binding to the MoS_2 nanomaterials at the higher concentrations is not significant enough to interfere adequately with our viability measurements. At the remaining concentrations, we observe no adsorption of the formazan crystal. Therefore, the MTT and WST-8 assay measurements in Figures 1 and 2 were corroborated with cell-free control experiments, ensuring the reliability of our cell viability data.

Having evaluated and substantiated the cytotoxicity effects that different exfoliated MoS_2 nanosheets can have on the A549 cells, we were also interested in comparing them with a graphene-related counterpart, since both MoS_2 and graphene sheets are inorganic, 2D nanomaterials that can be derived from layered bulk forms. Given that both *n*-Bu-Li and *t*-Bu-Li were shown to be much better intercalating agents than Me-Li at exfoliating the MoS_2 nanosheets, data from the *n*-Bu-Li and *t*-

Bu-Li exfoliated ones were included in Table 3 below. For comparison with the MoS_2 nanosheets, we chose graphene oxide nanoplatelets (GONPs) as the graphene counterpart nanomaterial. We have previously reported on the cytotoxicity of GONPs produced from the oxidation of stacked graphene nanofibers.[30]

Table 3. Comparison of MTT and WST-8 cell viability results obtained for GONPs, *n*-Bu-Li and *t*-Bu-Li exfoliated MoS_2.

MTT viability results (%)				WST-8 viability results (%)		
GONPs	*n*-Bu-Li	*t*-Bu-Li	**Concentration (μg/mL)**	GONPs	*n*-Bu-Li	*t*-Bu-Li
70.8	76.6	73.9	**6.25**	92.5	92.8	93.7
51.2	75.5	76.6	**25**	91.6	93.3	94.4
28.0	73.7	68.0	**100**	46.6	81.1	69.3
28.4	58.6	53.8	**200**	37.5	66.5	53.5
25.1	59.6	54.7	**400**	17.6	45.6	43.9

Overall, it is evident that the exfoliated MoS_2 nanosheets had a lessened cytotoxic impact on the cells as compared to the GONPs and, the disparity in their respective toxicity profiles became more apparent with increasing concentrations. Starting from 100 μg/mL onwards, the MoS_2 nanosheets were found to 1.4 – 2.6 times more toxic than the GONRs. We find that despite a high concentration of 400 μg/mL, the cytotoxic influence of the MoS_2 nanosheets were not as severe as compared with GONPs; approximately half of the cells incubated with the exfoliated MoS_2 retained their viability, unlike for the GONPs with only less than 25 % cell viability.

The dose-response results from the MTT and WST-8 assays, together with the characterization data have revealed that how well MoS_2 nanosheets are exfoliated plays a role in affecting their toxicity towards cells. The raman and XPS measurements, supported with appropriate electrochemical studies have shown that the *n*-Bu-Li and *t*-Bu-Li compounds act as better intercalating agents over Me-Li for the chemical exfoliation process of bulk MoS_2. Consequently when the exfoliated samples and bulk MoS_2 were assessed for their cytotoxic behavior, the A549 cells exposed to *n*-Bu-Li and *t*-Bu-Li exfoliated MoS_2 nanosheets experienced a stronger cytotoxic effect especially at higher concentrations. The toxicity impact of Me-Li exfoliated sample however, was greatly reduced and remained largely similar to that of the bulk MoS_2. Thus we have ascertained that the choice of Li-intercalatants is able to influence the extent of exfoliation and toxicity of the MoS_2 in the same order of *t*-Bu-Li > *n*-Bu-Li > Me-Li, strongly suggesting that well-exfoliated MoS_2 nanosheets can be correlated to greater *in-vitro* toxicity.

Well-exfoliated MoS_2 nanosheets can range from single- to few-layers and they offer a higher surface area, which is analogous to that of graphene-related nanomaterials. A recent study has uncovered the mechanism behind the cytotoxicity and antibacterial activity of graphene nanosheets which involved an insertion mode where the edge of the nanosheet is capable of inserting and cutting into the cell membrane, resulting in membrane stress leading to decreased cell viability.[31] It is plausible that well-exfoliated MoS_2 nanosheets which possess a large number of edge sites are able to interact with the A549 cells in the same manner causing cell death, thereby accounting for the greater cytotoxic profiles of the *t*-Bu-Li and *n*-Bu-Li exfoliated MoS_2 nanosheets over the Me-Li exfoliated ones.

Conclusions

While developments such as exfoliated nanoscale MoS_2 being used in bioapplications and sensing platforms are possible and should be further explored, we believe that their potential toxicity risks remains poorly understood. For that reason we have shown here for the first time, the dose-dependent response of MoS_2 nanosheets and how the extent of their exfoliation can influence their *in-vitro* toxicity, by conducting MTT and WST-8 assays. Three organolithium compounds – Me-Li, *n*-Bu-Li and *t*-Bu-Li were tested as intercalating agents in chemical exfoliation of bulk MoS_2. The toxicity assessments revealed that MoS_2 nanosheets exfoliated with *t*-Bu-Li and *n*-Bu-Li are significantly more cytotoxic than Me-Li exfoliated nanosheets; whilst the Me-Li exfoliated MoS_2 toxicity profile is largely similar to that of the bulk MoS_2. The characterization data confirmed that the *t*-Bu-Li and *n*-Bu-Li intercalating agents are more efficient at exfoliating MoS_2 than Me-Li, leading to a decrease in the number of MoS_2 layers as well as an increase in active surface area. Therefore, the cell toxicity results in conjunction with the characterization data demonstrates a strong correlation between well-exfoliated MoS_2 nanosheetsand their cytotoxic behavior, which can be influenced by the choice of intercalating agents. Given the fact that different TMDs show different toxicity[32], one could investigate the influence of intercalating agents on toxicity of WS_2 and WSe_2 as well. To bridge the transition between proof-of-concepts involving MoS_2 nanosheets to real-world applications, more research has to be done regarding the nanosafety of using inorganic MoS_2 nanomateirals to assess any possible risks associated to human health and the environment. What we have done in our study represents the first step taken towards appropriate nanotoxicological assessments of the MoS_2 nanomaterial.

Acknowledgements

M. P. thanks NAP fund (NTU) and Tier 1 fund (RGT 1/13). Z.S. thanks to the specific university research MSMT No. 20/2014.

Notes and references

[a] Division of Chemistry & Biological Chemistry, School of Physical and Mathematical Sciences, Nanyang Technological University, Singapore 637371
Fax: (65) 6791-1961
Email: pumera@ntu.edu.sg; pumera.research@gmail.com
[b] Institute of Chemical Technology, Department of Inorganic Chemistry, 166 28 Prague 6, Czech Republic.

1. H. Matte, A. Gomathi, A. K. Manna, D. J. Late, R. Datta, S. K. Pati, C. N. R. Rao, *Angew. Chem. Int. Ed.*, 2010, **49**, 4059.
2. K. S. Novoselov, D. Jiang, F. Schedin, T. J. Booth, V. V. Khotkevich, S. V. Morozov, A. K. Geim, *Proc. Natl. Acad. Sci. U. S. A.*, 2005, **102**, 10451.
3 A. Ambrosi, C. K. Chua, A. Bonanni, M. Pumera, *Chem. Rev.* 2014, **114**, 7150.
4. J. A. Wilson, A. D. Yoffe, *Adv. Phys.*, 1969, **18**, 193.
5. C. N. R. Rao, A. Nag, *Eur. J. Inorg. Chem.*, 2010, **2010**, 4244.
6. Y. F. Li, Z. Zhou, S. B. Zhang, Z. F. Chen, *J. Am. Chem. Soc.*, 2008, **130**, 16739.
7. S. Z. Butler, S. M. Hollen, L. Cao, Y. Cui, J. A. Gupta, H. R. Gutiérrez, T. F. Heinz, S. S. Hong, J. Huang, A. F. Ismach, E. Johnston-Halperin, M. Kuno, V. V. Plashnitsa, R. D. Robinson, R. S. Ruoff, S. Salahuddin, J. Shan, L. Shi, M. G. Spencer, M. Terrones, W. Windl, J. E. Goldberger, *ACS Nano*, 2013, **7**, 2898.
8. Y. Yoon, K. Ganapathi, S. Salahuddin, *Nano Lett.*, 2011, **11**, 3768.
9. B. Radisavljevic, A. Radenovic, J. Brivio, V. Giacometti, A. Kis, *Nat. Nanotechnol.*, 2011, **6**, 147.
10. C. Lee, H. Yan, L. E. Brus, T. F. Heinz, J. Hone, S. Ryu, *ACS Nano*, 2010, **4**, 2695.
11. G. Eda, H. Yamaguchi, D. Voiry, T. Fujita, M. Chen, M. Chhowalla, *Nano Lett.*, 2011, **11**, 5111.
12. A. Splendiani, L. Sun, Y. Zhang, T. Li, J. Kim, C.-Y. Chim, G. Galli, F. Wang, *Nano Lett.*, 2010, **10**, 1271.
13. M. Pumera, A. H. Loo, *Trends. Anal. Chem.* 2014, **61**, 49.
14. M. Pumera, Z. Sofer, A. Ambrosi, *J. Mater. Chem. A*, 2014, **2**, 8981.
15. S. Wu, Z. Zeng, Q. He, Z. Wang, S. J. Wang, Y. Du, Z. Yin, X. Sun, W. Chen, H. Zhang, *Small*, 2012, **8**, 2264.
16. H. Zhang, K. P. Loh, C. H. Sow, H. Gu, X. Su, C. Huang, Z. K. Chen, *Langmuir*, 2004, **20**, 6914.
17. C. Zhu, Z. Zeng, H. Li, F. Li, C. Fan, H. Zhang, *J. Am. Chem. Soc.*, 2013, **135**, 5998.
18 A. H. Loo, A. Bonanni, A. Ambrosi, M. Pumera, *Nanoscale* 2014, 10.1039/c4nr03795b
19. M. Pumera, *Chem Asian J*, 2011, **6**, 340.
20. K. J. Huang, L. Wang, Y. J. Liu, H. B. Wang, Y. M. Liu, L. L. Wang, *Electrochim. Acta,* 2013, **109**, 587.
21. A. Winchester, S. Ghosh, S. Feng, A. L. Elias, T. Mallouk, M. Terrones, S. Talapatra, *Appl. Mater. Interfaces*, 2014, **6**, 2125.
22. A. Ambrosi, Z. Sofer, M. Pumera, *Small*, 2014, DOI: 10.1002/smll.201400401
23. P. A. Bertrand, *Phys. Rev. B*, 1991, **44**, 5745.
24. P. Zhang, T. K. Sham, *Phys. Rev. Lett.*, 2003, **90**, 245502.
25. Y. Li, H. Wang, L. Xie, Y. Liang, G. Hong, H. Dai, *J. Am. Chem. Soc.*, 2011, **133**, 7296.
26. D. Merki, S. Fierro, H. Vrubel, X. L. Hu, *Chem. Sci.*, 2011, **2**, 1262.
27. N. A. Monteiro-Riviere, A. O. Inman, *Carbon*, 2006, **44**, 1070.
28. J. M. Wörle-Knirsch, K. Pulskamp, H. F. Krug, *Nano Lett.*, 2006, **6**, 1261.
29. L. Belyanskaya, P. Manser, P. Spohn, A. Bruinink, P. Wick, *Carbon*, 2007, **45**, 2643.
30. E. L. K. Chng, C. K. Chua, M. Pumera, *Nanoscale*, 2014, **6**, 10792.
31. Y. Tu, M. Lv, P. Xiu, T. Huynh, M. Zhang, M. Castelli, Z. Liu, Q. Huang, C. Fan, H. Fang, R. Zhou, *Nat. Nanotechnol.*, 2013, **8**, 594.
32 W. Z. Teo, E. L. K. Chng, M. Pumera, *Chem. Eur. J.* 2014, **20**, 9627.